

Local electronic structure of a single magnetic impurity in a superconductor

Michael E. Flatté

Department of Physics and Astronomy, University of Iowa, Iowa City, Iowa 52242

Jeff M. Byers

Naval Research Laboratory, Washington D.C. 20375

Abstract

The electronic structure near a single classical magnetic impurity in a superconductor is determined using a fully self-consistent Koster-Slater algorithm. Localized excited states are found within the energy gap which come in pairs whose energies are fully particle-hole symmetric. The spatial structure of the local density of states, however, can differ strongly for the two localized states of each pair. An approximate model with analytic solutions qualitatively reproduces the salient features of the numerical results.

Magnetic impurities have a dramatic effect on superconductivity. Most work on the experimental and theoretical effects of magnetic impurities have focused on bulk thermodynamic quantities, such as the reduction of the superconducting transition temperature T_c with increasing magnetic impurity concentration [1]. Theoretical approaches to treat the thermodynamic effects of impurities include Born scattering (Abrikosov-Gor'kov theory) [2] and approximate solutions to all orders in the impurity potential for classical [3] and quantum [4,5] spins. A key issue addressed in Ref. [3] was the evolution of localized excited states around impurities into an impurity band, eventually leading to gapless superconductivity at high enough impurity concentrations. The effects of impurities on bulk properties have also been treated within a strong-coupling formalism, but not self-consistently or beyond the Born approximation (e.g. Ref. [6]). Concern about bulk properties in the above and related work did not extend to properties very near the impurity.

Among the first properties calculated in the vicinity of an impurity were the structures of screening clouds around a charged impurity [7,8] and a magnetic impurity [8,9] in a superconductor (characterized by exponentially-decaying Friedel-like oscillations). Later Kummel calculated the spatial dependence of the order parameter near a magnetic impurity, although his calculation was not self-consistent [10]. Interest in local properties near impurities has been revived by advances in scanning tunneling microscopy (STM) near impurities embedded in a metallic medium [11].

Motivated by the possibility of measuring the local electronic structure near an impurity in a superconductor with an STM, the differential conductivity through an STM tip was calculated near impurities for superconductors with isotropic and anisotropic gaps within the Born approximation [12]. The differential conductivity measured at a point \mathbf{x} and voltage V and temperature T can be related to the local density of states at the tip location as follows:

$$\frac{dI(\mathbf{x}, V, T)}{dV} = \frac{1}{N_o} \int_{-\infty}^{\infty} d\omega \frac{\partial n(\omega)}{\partial \omega} \left(\frac{\text{Im}G(\mathbf{x}, \mathbf{x}; \omega = eV)}{\pi} \right). \quad (1)$$

Here e is the charge of the electron, $n(\omega)$ is the Fermi occupation function at temperature T , N_o is the density of states at the Fermi level, and dI/dV is in units of the normal-metal's

differential conductivity. The local density of states is the imaginary part of the retarded Green's function fully dressed by the interaction of the electronic system with the impurity. Within the Born approximation, then, the differential conductivity can be expressed in terms of the retarded homogeneous Green's functions of the superconductor, $g(\mathbf{x}, \mathbf{x}'; \omega)$ and $f(\mathbf{x}, \mathbf{x}'; \omega)$ (where f is the anomalous Green's function), in the following way:

$$\begin{aligned} \frac{dI(\mathbf{x}, V)}{dV} \propto \text{Im} \left[g(\mathbf{x}, \mathbf{x}; eV) \right. \\ \left. + g(\mathbf{x}, \mathbf{0}; eV)V_0g(\mathbf{0}, \mathbf{x}; eV) - f(\mathbf{x}, \mathbf{0}; eV)V_0f(\mathbf{0}, \mathbf{x}; eV) \right] \end{aligned} \quad (2)$$

where the impurity is at the location $\mathbf{0}$ in the solid and the non-magnetic impurity potential is $V_0\delta(\mathbf{x})$. For a BCS superconductor with an isotropic order parameter in a parabolic band, for ω much smaller than the Fermi energy,

$$\begin{aligned} g(\mathbf{x}, \mathbf{x}'; \omega) &= -\frac{\pi N_o}{k_F r} e^{-\sqrt{\Delta^2 - \omega^2} k_F r / \pi \xi \Delta} \left(\cos k_F r + \frac{\omega}{\sqrt{\Delta^2 - \omega^2}} \sin k_F r \right) \\ f(\mathbf{x}, \mathbf{x}'; \omega) &= -\frac{\pi N_o \Delta}{k_F r \sqrt{\Delta^2 - \omega^2}} e^{-\sqrt{\Delta^2 - \omega^2} k_F r / \pi \xi \Delta} \sin k_F r \end{aligned} \quad (3)$$

where $r = |\mathbf{x} - \mathbf{x}'|$, Δ is the order parameter, and ξ is the coherence length. These expressions are valid for ω above and below Δ so long as the imaginary parts of both f and g are multiplied by $\text{sgn}\omega$.

The Born approximation calculation would not yield any localized states around the impurity, and does not consider the effect of the change in electronic structure on the local order parameter $\Delta(\mathbf{x})$. Recent preliminary STM results indicate certain features of the LDOS near a magnetic impurity [13]: (1) discrete states are evident within the energy gap whose LDOS is asymmetric, and (2) the LDOS becomes indistinguishable from the bulk density of states within a distance greater than the Fermi wavelength but much less than the coherence length. A calculation beyond the Born approximation where the order parameter is self-consistently determined would be required to explain these results.

We will present a fully self-consistent calculation of the local electronic structure near a magnetic impurity which is based on a Koster-Slater-like Green's function technique rather

than the Bogoliubov-de-Gennes (BdG) equations [14]. The BdG equations are Schrödinger-like equations for the electron and hole components of the quasiparticle wavefunctions. The localized states of a vortex core in a superconductor and other properties revealed by the LDOS were calculated self-consistently using the BdG equations [15,16]. These results were compared with a measurement of a single vortex by an STM on superconducting NbSe₂ [17]. The BdG equations were successfully used again to explain the STM observations of the vortex lattice [18].

Since the original application of the Green's function algorithm to localized vibrational modes [19], it has been applied to numerous problems including conduction electrons in metals [20] and impurity states in magnets [21], but not to superconductors. To place this algorithm in context we will contrast it with the BdG equations. To find the quasiparticle wavefunctions, typically the inhomogeneity is placed in a sphere of radius R with appropriate boundary conditions. The value of R is determined by the spectral resolution necessary for accurately evaluating determining the order parameter self-consistently and the spectral width of features measurable by (for example) the STM. The typical complications resulting from approximating an infinite system by a finite-size system apply, such as discrete states above the energy gap and the heavy investment of computer time required for large values of R .

The Green's function method works within a sphere whose radius is determined by the range of the inhomogeneous potential. In essence we shall invert the Dyson equation in real space. The Dyson equation for an inhomogeneity in a superconductor, the Gor'kov equations [22], can be written as:

$$\int d\mathbf{x}'' [\delta(\mathbf{x} - \mathbf{x}'') - \mathbf{g}_\sigma(\mathbf{x}, \mathbf{x}'', \omega) \mathbf{V}(\mathbf{x}'')] \mathbf{G}_\sigma(\mathbf{x}'', \mathbf{x}; \omega) = \mathbf{g}_\sigma(\mathbf{x}, \mathbf{x}'; \omega) \quad (4)$$

where

$$\mathbf{g}_\sigma(\mathbf{x}, \mathbf{x}'; \omega) = \begin{pmatrix} g_\sigma(\mathbf{x}, \mathbf{x}'; \omega) & f_\sigma(\mathbf{x}, \mathbf{x}'; \omega) \\ f_\sigma^*(\mathbf{x}, \mathbf{x}', -\omega) & -g_\sigma^*(\mathbf{x}, \mathbf{x}', -\omega) \end{pmatrix}, \quad (5)$$

the same relationship exists among \mathbf{G}_σ , G_σ and F_σ , and

$$\mathbf{V}(\mathbf{x}'') = \begin{pmatrix} \sigma V_S(\mathbf{x}'') + V_0(\mathbf{x}'') & \delta\Delta(\mathbf{x}'') \\ \delta\Delta(\mathbf{x}'') & \sigma V_S(\mathbf{x}'') - V_0(\mathbf{x}'') \end{pmatrix}. \quad (6)$$

$\delta\Delta(\mathbf{x}) = \Delta(\mathbf{x}) - \Delta_o$, where $\Delta(\mathbf{x})$ is the position-dependent order parameter and Δ_o is the order parameter of the homogeneous superconductor. $V_S(\mathbf{x})$ is a localized, spin-dependent potential, such as one originating from a classical spin. $V_0(\mathbf{x})$ is a localized non-magnetic potential. The quantization direction of the superconductor's spins ($\sigma = \pm 1/2$) is chosen parallel to the direction of the classical spin. g_σ is given by Eqs. (3) with N_o labelling the density of states for each spin. $G_\sigma \neq G_{-\sigma}$ due to the differences in the potential in Eq. (6). The self-consistency equation is

$$\delta\Delta(\mathbf{x}) = \gamma \sum_{\sigma} \int_{-\infty}^{\infty} d\omega n(\omega) \text{Im} F_{\sigma}(\mathbf{x}, \mathbf{x}; \omega) - \Delta_o, \quad (7)$$

where γ is the pairing strength.

One strength of this formalism is its reliance on the short-range nature of the inhomogeneous potential. Solution of Eq. (4) requires inverting the frequency-dependent real-space matrix $\mathbf{M}(\omega) = \delta(\mathbf{x} - \mathbf{x}') - \mathbf{g}_{\sigma}(\mathbf{x}, \mathbf{x}'; \omega) \mathbf{V}(\mathbf{x}')$. For \mathbf{x}' 's where $\mathbf{V}(\mathbf{x}')$ is negligible, that portion of $\mathbf{M}(\omega)$ is triangular and trivially invertible. Hence the numerical complexity of inverting $\mathbf{M}(\omega)$ is governed by the range of $\mathbf{V}(\mathbf{x})$. The radius of the sphere the system is solved in is governed by the range of the longest-range potential, which in this paper will be $\delta\Delta(\mathbf{x})$.

As a special case of Eq. (4), the energies of the localized states within the gap correspond to those ω where $\det \mathbf{M}(\omega) = 0$. We model the impurity with a Gaussian $V_S(\mathbf{x})$ of range k_F^{-1} . Figure 1 shows the dependence of the localized state energies for the first two angular momentum channels on the strength of the magnetic potential, $v_s = \pi N_o |\sigma \int d\mathbf{x} V_S(\mathbf{x})|$. For $V_0 = 0$, the Eqs. (4)-(7) are unchanged by the transformation $\omega \rightarrow -\omega$ and $s \rightarrow -s$ so the localized excited state energies must come in symmetric pairs around $\omega = 0$ [23]. The state near $+\Delta_o$ for small v_s is the spin state attracted to the classical spin, which we will label up (\uparrow). As the potential strength increases, the excitation energy of each angular momentum state ℓ decreases, at some critical value ($v_{s\ell}^*$) vanishes, and then begins to increase. This qualitative behavior of the excitation energies can be extracted from the Shiba model [3],

where the magnetic potential is modeled by a delta function at the impurity site. The zeros of $M(\omega)$ are found, neglecting the component of $\text{Reg}(\mathbf{x}, \mathbf{x}'; \omega)$ which is symmetric for $\omega \rightarrow -\omega$. These energies are shown in Figure 1.

The spectral weight of the up state is strongly concentrated at the origin, while that of the down state is pushed away from the origin. Figure 2 shows the calculated angular momentum $\ell = 0$ spectral weights for two values of v_s , indicating that the asymmetry of the spatial structure of the spectral weights becomes more pronounced with increasing v_s . Also shown are $\ell = 1$ spectral weights for $v_s = 0.875$. The asymmetric localized-state spectral weights produce differential conductivities which are asymmetric as well [24]. Figure 3 shows differential conductivities for $v_s = 1.75$ at three locations — right at the impurity, k_F^{-1} away, and $10k_F^{-1}$ away. By $10k_F^{-1}$ the spectrum has recovered to the homogeneous spectrum. The differential conductivity farther away can be easily recovered by constructing the self-consistent \mathbf{T} -matrix $\mathbf{V}(\mathbf{x}')\delta(\mathbf{x}' - \mathbf{x}'') + \mathbf{V}(\mathbf{x}')\mathbf{G}(\mathbf{x}', \mathbf{x}''; \omega)\mathbf{V}(\mathbf{x}'')$ directly from the dressed Green's functions. The spatial dependence of the differential conductivity far away from the impurity is qualitatively identical to the Born result [12].

The asymmetric behavior of the up and down spectral weights does not emerge from the model of Ref. [3], which implies identical spatial dependences of the spectral weights for the up and down states. As pointed out by Koster and Slater [20], proper treatment of the symmetric real part of $g(\mathbf{0}, \mathbf{0}; \omega)$ is essential for obtaining the local electronic properties around an impurity. The proper approximation for the real symmetric part of the Green's function is to average it over a small volume given by the range of the potential modeled by the delta function. We therefore introduce a new parameter into the Shiba model, α , which is the ω -symmetric part of $\text{Re}\langle g(\mathbf{0}, \mathbf{0}; \omega = 0) \rangle / \pi N_o$. The brackets indicate that $g(\mathbf{0}, \mathbf{x}; \omega = 0)$ has been averaged over a small volume. For $\alpha \neq 0$ the ratio of the spectral weight of the up state at the impurity, $A_{\uparrow}(\mathbf{0})$, to the spectral weight of the down state at the impurity, $A_{\downarrow}(\mathbf{0})$, is

$$\frac{A_{\uparrow}(\mathbf{0})}{A_{\downarrow}(\mathbf{0})} = \frac{1 + 2\alpha v_s + (1 + \alpha^2)v_s^2}{1 - 2\alpha v_s + (1 + \alpha^2)v_s^2}. \quad (8)$$

The introduction of α does not change the localized state energies qualitatively.

We now discuss the structure of $\Delta(\mathbf{x})$. Figure 4 shows $\delta\Delta(\mathbf{x})$'s for two values of v_s . While oscillating with wavelength $\sim \pi k_F^{-1}$, $\delta\Delta(\mathbf{x})$ falls off to a negligible potential within $10k_F^{-1}$. This justifies performing the numerical calculation in a sphere of that radius. A typical radial grid of 100 points provides a numerically robust solution. The self-consistent solution also depends on the value of $N_o\Delta_o/k_F^3$, which for niobium is 10^{-3} [25].

As shown in Figure 4, for large values of v_s , $\Delta(\mathbf{x} = \mathbf{0}) < 0$. Sign changes in Δ , as seen in pair tunneling, have been suggested for magnetic impurities in the barriers of Josephson junctions [26]. Our sign change in $\Delta(\mathbf{0})$ occurs (at $T = 0$) precisely at v_{s0}^* . The contribution to $\Delta(\mathbf{0})$ from the up state has the opposite sign to that from the down state. For small v_s , the down state's energy is negative and the up state's energy is positive, so the down state contributes to $\Delta(\mathbf{x})$ (see Eq. (7)). When $v_s > v_{s0}^*$ the states reverse and the up state contributes to $\Delta(\mathbf{x})$. At this point $\Delta(\mathbf{0})$ changes discontinuously. $\Delta(\mathbf{0})$ as a function of v_s is shown in the insert of Figure 4. At $T > 0$ the transition would be smoothed somewhat.

The behavior of $\Delta(\mathbf{0})$ as a function of v_s can be tied to the crossing of the energy levels in Fig. 1 with the following picture. For small v_s the pair closest to the impurity is polarized by the spin. The up electron is pulled closer to the spin and the down electron is pushed away. This weakens the pair and allows for local pair-breaking excitations of energy less than $2\Delta_o$. For $v_s > v_{s0}^*$ the spin potential is so strong that the pair is broken in the ground state of the superconductor. The ground state has a spin up quasiparticle localized near the impurity and a spin down quasiparticle farther away. In support of this picture we find that exciting the low-energy states for $v_s > v_{s0}^*$ *increases* $\Delta(\mathbf{0})$, whereas excitation of quasiparticles typically *reduces* $\Delta(\mathbf{x})$. Also, exciting the low-energy states *reduces* the induced spin of the superconductor at the impurity. For $v_s > v_{s0}^*$, exciting the two low-energy states causes a pair to enter the condensate. We note that this picture should have implications for the theory of gapless superconductivity, which is now based on the formation of impurity bands through hybridization of single-quasiparticle excited states around impurities.

M.E.F. wishes to acknowledge the Office of Naval Research's Grant No. N00014-96-1-1012. J.M.B. wishes to acknowledge an N.R.C. Fellowship.

REFERENCES

- [1] B. T. Matthias, H. Suhl, and E. Corenzwit, Phys. Rev. Lett. **1**, 92 (1958), C. Herring, Physica **24**, S 184 (1958) and H. Suhl and B. T. Matthias, Phys. Rev. **114**, 977 (1959).
- [2] A. A. Abrikosov and L. P. Gor'kov, Zh. Eksp. Teor. Fiz. **39**, 1781 (1962) (Soviet Phys. JETP **12**, 1243 (1961)).
- [3] H. Shiba, Prog. Theor. Phys. **40**, 435 (1968).
- [4] J. Zittartz and E. Müller-Hartmann, Z. Physik **232**, 11 (1970), E. Müller-Hartmann and J. Zittartz, Z. Physik **234**, 58 (1970).
- [5] E. Müller-Hartmann and J. Zittartz, Phys. Rev. Lett. **26**, 428 (1971).
- [6] F. Marsiglio, J.P. Carbotte, A. Puchkov, and T. Timusk, Phys. Rev. B **53**, 9433 (1996).
- [7] R. Prange, Phys. Rev. **129**, 2495 (1963).
- [8] J. P. Hurault, Journal de Physique **26**, 252 (1965).
- [9] P.W. Anderson and H. Suhl, Phys. Rev. **116**, 898 (1959).
- [10] R. Kummel, Phys. Rev B **6**, 2617 (1972).
- [11] M.F. Crommie, C.P. Lutz, and D.M. Eigler, Nature (London), **363**, 524 (1993). Y. Hasegawa and P. Avouris, Phys. Rev. Lett. **71**, 1071 (1993).
- [12] J.M. Byers, M.E. Flatté, D.J. Scalapino, Phys. Rev. Lett. **71**, 3363 (1993).
- [13] A. Yazdani, C. P. Lutz and D. E. Eigler, unpublished.
- [14] See, e. g., P. G. de Gennes, *Superconductivity of Metals and Alloys* (Addison-Wesley, Reading, MA 1989).
- [15] J. D. Shore, M.Huang, A. T. Dorsey and J. P. Sethna, Phys. Rev. Lett. **62**, 3089 (1989).
- [16] F. Gygi and M. Schlüter, Phys. Rev. B **41**, 822 (1990) and F. Gygi and M. Schlüter,

- Phys. Rev. B **43**, 7609 (1991).
- [17] H. F. Hess, R. B. Robinson, R. C. Dynes, J. M. Valles, Jr., and J. V. Waszicak, Phys. Rev. Lett. **62**, 214 (1990); J. Vac. Sci. Technol. A **8**, 450 (1990).
- [18] H. Hess, R. B. Robinson, and J. V. Waszczak, Phys. Rev. Lett. **64**, 2711 (1990) and F. Gygi and M. Schlüter, Phys. Rev. Lett. **65**, 1820 (1990).
- [19] E. W. Montroll and R.B. Potts, Phys. Rev. **100**, 525 (1955).
- [20] G.F. Koster and J.C. Slater, Phys. Rev. **95**, 1167 (1954). G.F. Koster and J.C. Slater, Phys. Rev. **96**, 1208 (1954).
- [21] T. Wolfram and J. Callaway, Phys. Rev. **130**, 2207 (1963).
- [22] See A.A. Abrikosov, L.P. Gor'kov, and I.E. Dzyaloshinski, *Methods of Quantum Field Theory in Statistical Physics* (Dover, New York, 1963).
- [23] Even when $V_0 \neq 0$ the discrete-state energies come in symmetric pairs.
- [24] We expect the local electronic structure around an impurity on a surface, which is measurable by STM, to be qualitatively the same as the structure around an impurity embedded in the bulk.
- [25] K. -H. Hellwege and J. L. Olsen, eds., *Landolt-Börnstein* **13c** (Springer, Berlin, 1984).
- [26] See references in M. Sigrist and T.M. Rice, Rev. Mod. Phys. **67**, 503 (1995).

FIGURES

FIG. 1. Solid lines indicate the self-consistently calculated localized excited state energies for angular momentum channels $\ell = 0$ and 1. The analytic model of Ref. [3] is shown by the dashed lines. The positive energy states for small magnetic potential (v_s) are concentrated near the impurity (spin up), while the negative energy states are concentrated farther away (spin down). At a critical value of $v_s = v_{s0}^*$, the up $\ell = 0$ state crosses to negative energy and the down $\ell = 0$ state crosses to positive energy, indicating a change in the character of the ground state. The kink evident in the solid line is real, and due to the discontinuous change (at $T = 0$) in $\Delta(\mathbf{x})$ at v_{s0}^* .

FIG. 2. Spectral weights for the $\ell = 0$ up and down states as a function of position for two values of the magnetic potential. Also shown are the spectral weights for the up and down states for $\ell = 1$ for $v_s = 0.875$.

FIG. 3. Differential conductivity (dI/dV), relative to the normal metal at three distances (in units of k_F^{-1}) from the impurity for $v_s = 1.75$, showing the evolution of the spectrum from one dominated by the localized states near $r = 0$ to one dominated by the bulk spectrum at $r = 10$. The curve at $r = 0$ has been shrunk by a factor of two so that it can appear on the same scale as the other two curves. The presence of the large peak near the origin on the negative-frequency side of the spectrum indicates that the impurity is strong ($v_s > v_{s0}^*$). dI/dV has been evaluated from Eq. (1) with $\beta = 7.5/\Delta_o$, which for niobium corresponds to $T \sim 2\text{K}$.

FIG. 4. Change in the local order parameter, $\delta\Delta(\mathbf{x})$, for two values of the magnetic potential. The change becomes negligible beyond $10k_F^{-1}$. (Insert) Order parameter at the impurity, $\Delta(\mathbf{0})$, as a function of v_s , indicating a discontinuous change at v_{s0}^* .

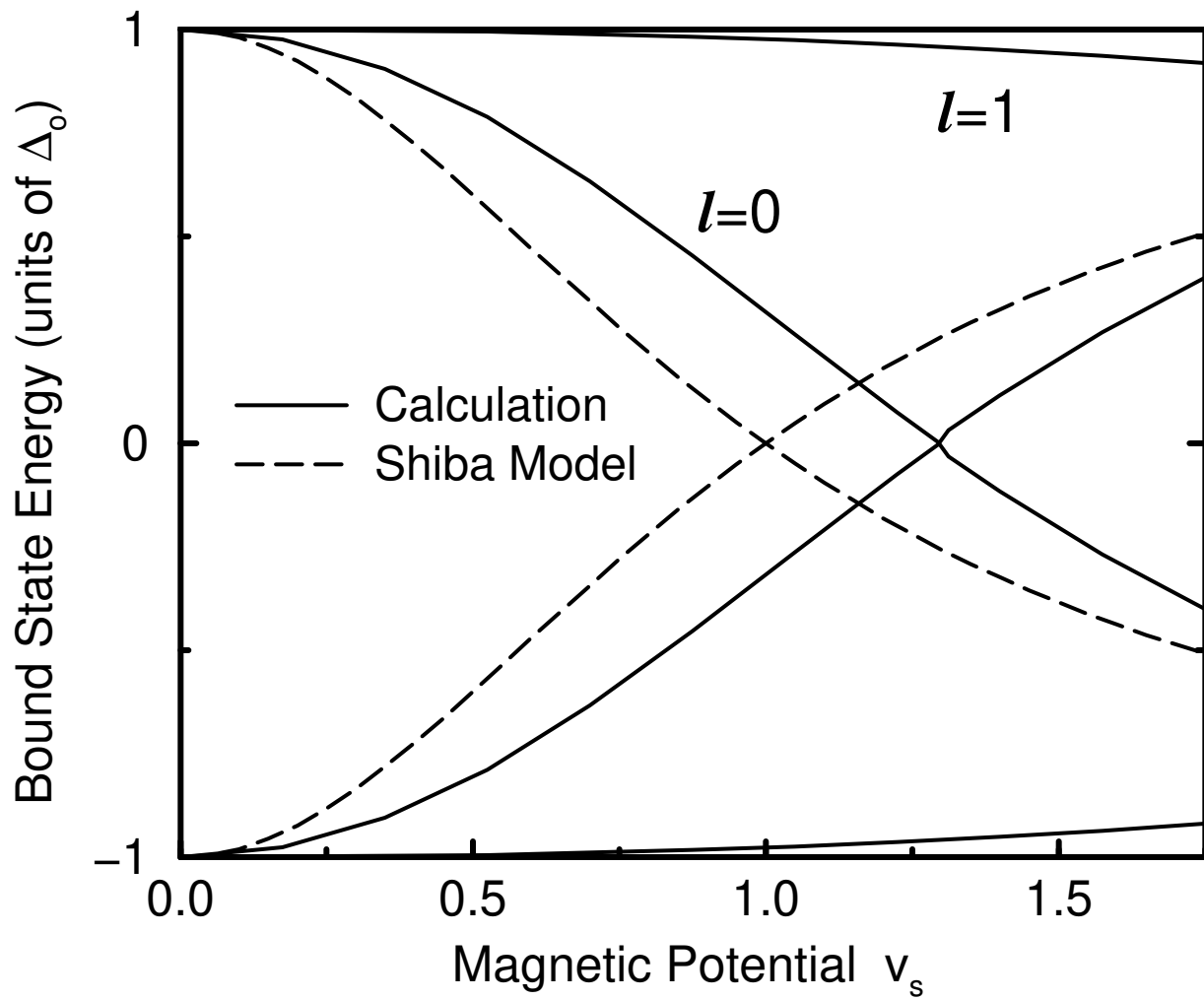


Fig. 1

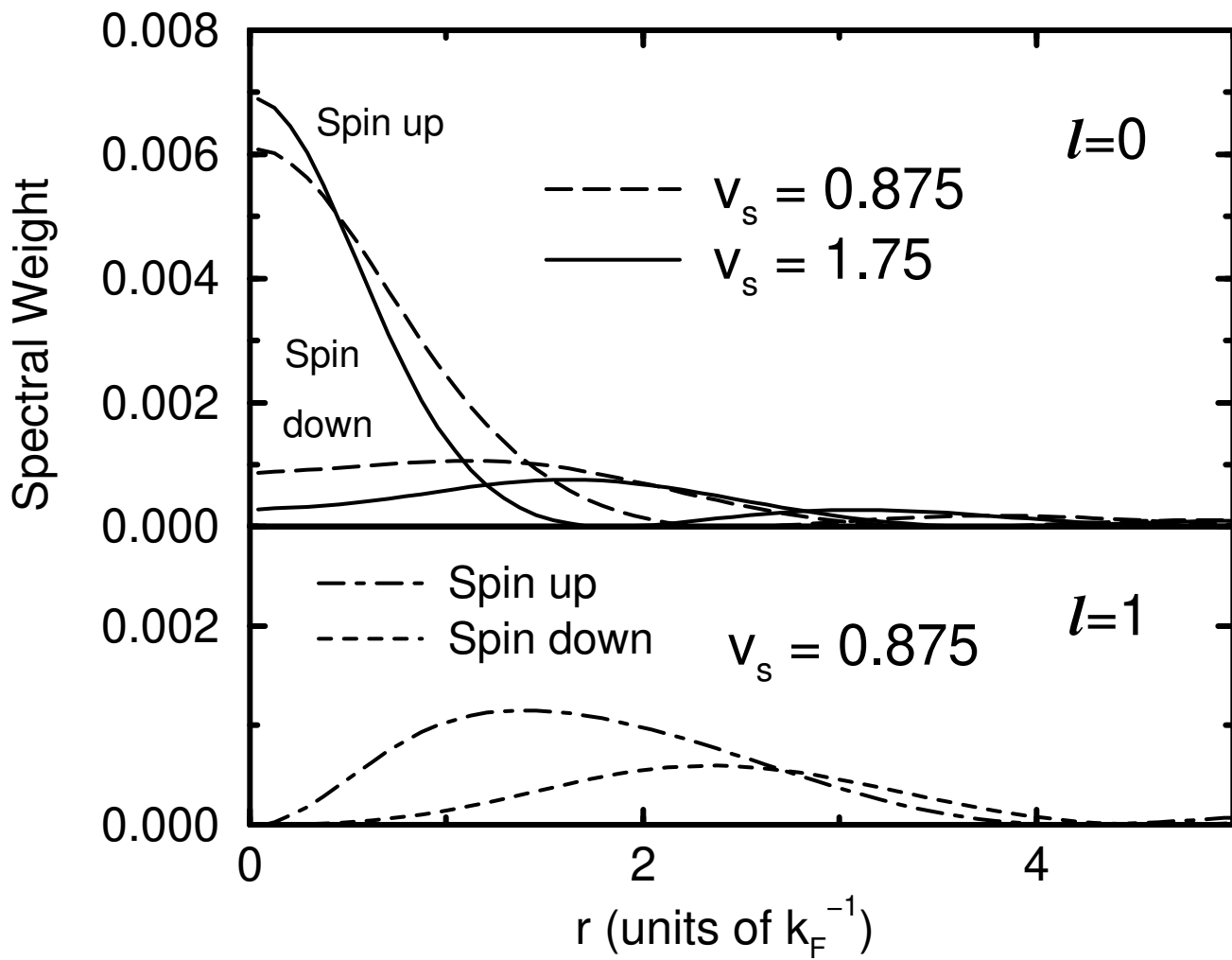


Fig. 2

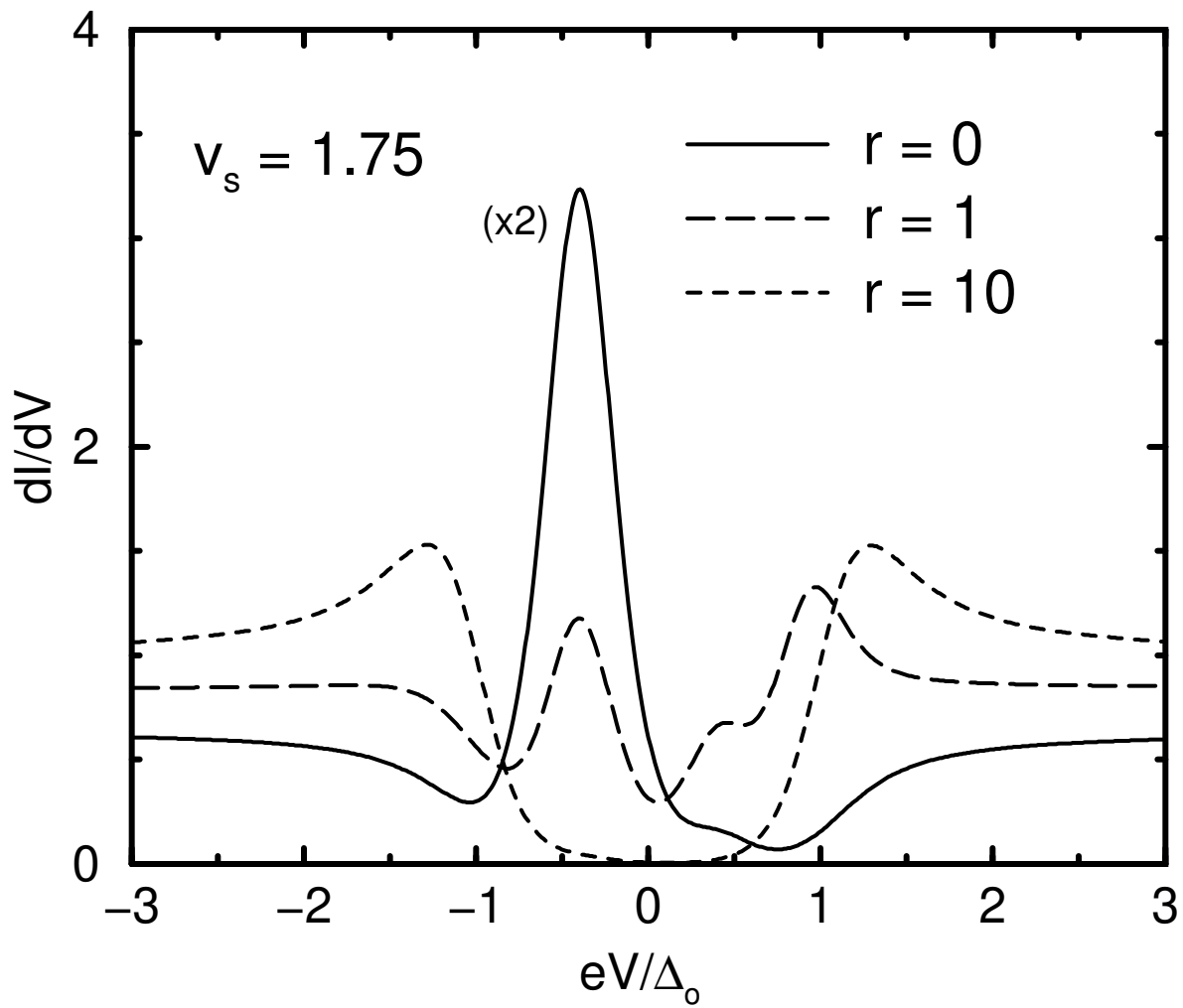


Fig. 3

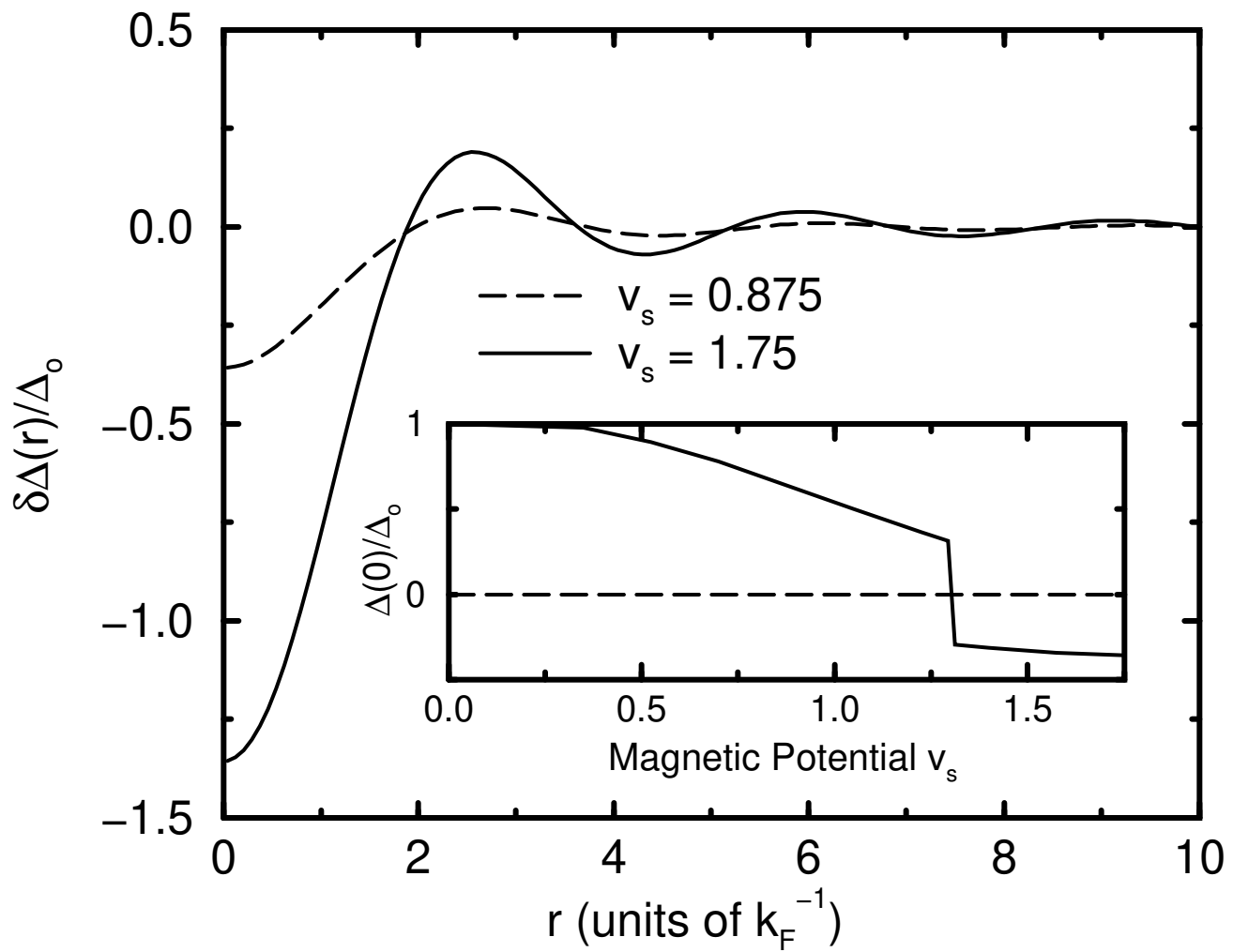


Fig. 4